Identification of the Active Site Acid/Base Catalyst in a Bacterial Fumarate Reductase: A Kinetic and Crystallographic Study†

Mary K. Doherty,‡ Sara L. Pealing,‡,§ Caroline S. Miles,§ Ruth Moysey,‡ Paul Taylor,§ Malcolm D. Walkinshaw,§ Graeme A. Reid,§ and Stephen K. Chapman*,‡

Department of Chemistry, University of Edinburgh, West Mains Road, Edinburgh EH9 3JJ, U.K., and Institute of Cell and Molecular Biology, University of Edinburgh, Mayfield Road, Edinburgh EH9 3JR, U.K.

Received April 17, 2000; Revised Manuscript Received May 31, 2000

ABSTRACT: The active sites of respiratory fumarate reductases are highly conserved, indicating a common mechanism of action involving hydride and proton transfer. Evidence from the X-ray structures of substrate-bound fumarate reductases, including that for the enzyme from *Shewanella frigidimarina* [Taylor, P., Pealing, S. L., Reid, G. A., Chapman, S. K., and Walkinshaw, M. D. (1999) *Nat. Struct. Biol*. *6*, 1108−1112], indicates that the substrate is well positioned to accept a hydride from N5 of the FAD. However, the identity of the proton donor has been the subject of recent debate and has been variously proposed to be (using numbering for the *S. frigidimarina* enzyme) His365, His504, and Arg402. We have used site-directed mutagenesis to examine the roles of these residues in the *S. frigidimarina* enzyme. The H365A and H504A mutant enzymes exhibited lower k_{cat} values than the wild-type enzyme but only by factors of 3−15, depending on pH. This, coupled with the increase in K_m observed for these enzymes, indicates that His365 and His504 are involved in Michaelis complex formation and are not essential catalytic residues. In fact, examination of the crystal structure of *S. frigidimarina* fumarate reductase has led to the proposal that Arg402 is the only plausible active site acid. Consistent with this proposal, we report that the R402A mutant enzyme has no detectable fumarate reductase activity. The crystal structure of the H365A mutant enzyme shows that, in addition to the replacement at position 365, there have been some adjustments in the positions of active site residues. In particular, the observed change in the orientation of the Arg402 side chain could account for the decrease in k_{cat} seen with the H365A enzyme. These results demonstrate that an active site arginine and not a histidine residue is the proton donor for fumarate reduction.

Fumarate reductases enable bacteria to respire anaerobically with fumarate as a terminal electron acceptor. In most cases these enzymes are membrane-bound complexes, closely related to succinate dehydrogenase, but in *Shewanella* the fumarate reductase is a soluble, periplasmic, tetraheme flavocytochrome c_3 (Fcc_3,[1] M_r 63 800). The gene encoding Fcc_3 has been cloned and sequenced (Swissprot entry FRDA_SHEPU), and the protein product has been shown to be a novel respiratory fumarate reductase (*1*, *2*).

Fumarate reductases from several other bacteria have been identified as complexes of three or, more commonly, four subunits that are anchored to the inner face of the cytoplasmic membrane (*3*, *4*). The largest of these, FrdA, is a flavoprotein containing the site of substrate reduction, and this is tightly associated with the FrdB subunit which contains three iron−sulfur centers that feed electrons to the flavin. These two subunits are very closely related to succinate dehydrogenase subunits that catalyze the reverse reaction. The A and B subunits are peripheral membrane proteins that are associated with smaller, integral membrane proteins that transfer electrons from the lipophilic hydrogen carrier, menaquinone, to the iron−sulfur centers. Fumarate reductase from *Escherichia coli* contains two membrane anchor subunits, FrdC and FrdD, that are devoid of prosthetic groups (*3*) whereas the equivalent enzyme from *Wolinella succinogenes* contains a single membrane subunit that is a diheme cytochrome *b* (*4*).

In contrast to these cytoplasmic membrane enzymes, Fcc_3 is a soluble, single-chain enzyme found in the periplasm (*5*). Despite the differences in architecture and location, its function has been shown to be analogous to that of the membrane-bound enzymes since disruption of the gene encoding Fcc_3 resulted in the specific loss of the ability to respire with fumarate as the electron acceptor (*6*). The recently determined crystal structure of Fcc_3 (*7*−*10*) shows it to be composed of three domains. These have been termed the cytochrome domain, the flavin domain, and the clamp domain (*7*). The flavin binding domain is clearly related by sequence to the flavoprotein subunits of the membrane-bound fumarate reductases and succinate dehydrogenases (*2*), and all of the amino acid residues that have been implicated in substrate binding and catalysis, on the basis of chemical modification and mutagenesis experiments, are conserved.

† This work was funded by the U.K. Biotechnology and Biological Sciences Research Council, BBSRC. M.K.D. and R.M. acknowledge studentships from the BBSRC and EPSRC. We thank SRS Daresbury for use of synchrotron data collection facilities.

* Corresponding author: e.mail, S.K.Chapman@ed.ac.uk; fax/phone, (44) 131 650 4760.

‡ Department of Chemistry, University of Edinburgh.

§ Institute of Cell and Molecular Biology, University of Edinburgh.

[1] Abbreviations: Fcc_3, flavocytochrome c_3; H365A, histidine 365 → alanine mutation; H504A, histidine 504 → alanine mutaion; R402A, arginine 402 → alanine mutation; FAD, flavin adenine dinucleotide.

10.1021/bi000871l CCC: $19.00
Published on Web 08/09/2000

One particular histidine residue (His365 in Fcc_3, equivalent to His232 in *E. coli* fumarate reductase) has been proposed as a possible active site acid/base catalyst for fumarate reduction/succinate oxidation (*11*, *12*). In *E. coli* fumarate reductase, the substitution of His232 by serine resulted in an enzyme which retained 25% of its fumarate reductase activity but only 2% of its succinate dehydrogenase activity (*12*). Such data are consistent with this residue having a significant but nonessential role in enzyme activity. Retention of 25% of the wild-type fumarate reductase activity clearly indicates that an alternative proton donor must be operational. The recently determined high-resolution crystal structure of Fcc_3 supports the idea that His365 is unlikely to be the active site acid (*7*). First, the structure shows that N5 of His365 is hydrogen bonded to a backbone amide group, indicating that the imidazole ring must be neutral. Second, N3 of His365 is hydrogen bonded to one of the carboxylate groups of the substrate with the imidazole ring too far (4.88 Å) from the C3 carbon to which the proton must be donated (*7*).

The possibility of an alternative histidine (residue 504 in the Fcc_3 sequence) acting as the active site acid has been suggested on the basis of the recent structure of an isozyme of Fcc_3 known as iron-induced flavocytochrome c_3 (*10*). There is no supporting evidence for this suggestion since the active site in this structure is unoccupied. Indeed, the suggestion is incompatible with evidence from the structures of the *E. coli* fumarate reductase (*3*) and the other *Shewanella* enzymes (*7*, *8*), all of which have substrate- or inhibitor-like molecules bound at the active site. In these cases the structures indicate a role in the binding of substrate but not in the donation of a proton to substrate C3. The highest resolution Fcc_3 structure (*7*) clearly indicates that Arg402 is the most likely active site acid. This is supported by the structure of the related Fcc_3 from *Shewanella putrefaciens* MR-1 (*9*).

To further investigate the nature of the active site acid catalyst, we have examined the roles of residues His365, Arg402, and His504 by substituting each by alanine and in addition have made the H365A:H504A double substitution. In the present paper we describe the kinetic characterization of these mutant enzymes. In addition, we report the 1.8 Å resolution crystal structure of H365A Fcc_3.

MATERIALS AND METHODS

DNA Manipulation, Strains, Media, and Growth. The mutant enzymes H365A Fcc_3, R402A Fcc_3, and H504A Fcc_3 were generated by site-directed mutagenesis using the method described by Kunkel and Roberts (*13*). The *fccA* coding sequence was cloned into the phagemid vector pTZ18R (*14*) on an ~1.8 kbp *Eco*RI/*Hin*dIII fragment (*6*) to provide the template.

Mutagenic oligonucleotides GTATATCCAAGCTGCTCCAACACTATCTG (which substitutes histidine 365 with alanine), CGAAATTACTACTGCTGATAAAGCATC (which substitutes arginine 402 with alanine), and GTTACACCTGGTGTTGCTCACACTATGGGTG (which substitutes histidine 504 with alanine) were obtained from PE-Applied Biosystems U.K. Mismatched bases are underlined. Single-stranded DNA was screened for the required mutations by dideoxy chain termination sequencing (*15*) using the Sequenase version 2.0 kit (United States Biochemicals). To verify that no secondary mutations had been introduced, the mutated *fccA* coding sequences were fully sequenced from single-stranded DNA: *H365A fccA* as above and *R402A* and *H504A fccA* using a Perkin-Elmer ABI Prism 377 DNA sequencer.

To enable expression of H365A, R402A, and H504A Fcc_3, the modified coding sequences were cloned individually into the IPTG-inducible, broad-host range expression vector pMMB503EH (*16*) on an ~1.8 kbp *Eco*RI/*Hin*dIII fragment to give pCM15, pCM68, and pCM67, respectively. Following transformation of *E. coli* SM10 (*17*), the above plasmids were transferred to the Δ*fccA Shewanella frigidimarina* strain EG301 (*6*) by conjugation. Recombinant wild-type Fcc_3 was expressed in the same manner (*6*). To generate H365A:H504A Fcc_3, an ~1.1 kbp *Nhe*I/*Mfe*I fragment was excised from pCM67 (H504A *fccA*/pMMB503EH) and replaced with the corresponding fragment from pCM14 (H365A *fccA*/pTZ18R). Expression was as described above.

Protein Purification and Kinetic Analysis. Wild-type and mutant forms of Fcc_3 were purified as previously reported (*1*). Protein samples for crystallization were subjected to an additional purification step using FPLC with a Mono Q column as described by Pealing et al. (*18*). Protein concentrations were determined using the Soret band absorption coefficient for the reduced enzyme (752.8 mM^{-1} cm^{-1} at 419 nm) (*1*).

The FAD content of recombinant Fcc_3 was determined using the method of Macheroux (*19*), and all steady-state rate constants were corrected for the percentage of FAD present.

The steady-state kinetics of fumarate reduction were followed at 25.0 ± 0.1 °C as described by Turner et al. (*20*). The fumarate-dependent reoxidation of reduced methyl viologen was monitored at 600 nm using a Shimadzu UV-PC 1201 spectrophotometer. To ensure anaerobicity the spectrophotometer was housed in a Belle Technology glovebox under a nitrogen atmosphere with the O_2 level maintained below 5 ppm. Assay buffers contained 0.45 M NaCl and 0.2 mM methyl viologen and were adjusted to the appropriate pH values using 0.05 M HCl or NaOH as follows: Tris·HCl (pH 7.0−9.0), MES/NaOH (pH 5.4−6.8), CHES/NaOH (pH 8.6−10), and CAPS/NaOH (pH 9.7−11.1). The viologen was reduced by addition of sodium dithionite until an absorbance reading of around 1 was obtained (corresponding to around 80 μM reduced methyl viologen). The concentration of reduced methyl viologen could be varied between 100 and 20 μM with no effect on the rate of reaction. Fumarate was added to give a range of concentrations (0−350 μM), and the reaction was initiated by addition of a known concentration of enzyme.

Kinetic parameters K_m and k_{cat} were determined from the steady-state results using nonlinear regression analysis (Microcal Origin software).

Crystallization and Refinement. Crystallization was carried out by hanging drop vapor diffusion at 4 °C in Linbro plates. Crystals were obtained with a well solution comprising 100 mM Tris·HCl, pH 7.4 (measured at 25 °C), 80 mM NaCl, 17−20% PEG 8000, and 10 mM fumarate. Hanging drops of 4 μL were prepared by adding 2 μL of 6 mg/mL protein (in 10 mM Tris·HCl, pH 8.4) to 2 μL of well solution. Needles of up to 1 × 0.2 × 0.2 mm were formed after about 2 weeks.

Crystals were immersed in well solution containing 23% glycerol as cryoprotectant, before being mounted in loops

Table 1: Refinement Statistics

refinement	24.0−1.8 Å
total no. of reflections	265 858
unique reflections	54 333
completeness (%)	90.7
$\langle I\rangle/\langle\sigma(I)\rangle$	13.8
R_{merge} (%)[a]	4.9
R_{merge} in outer shell (1.83−1.80) (%)	11.7
R_{cryst} (%)[b]	18.14
R_{free} (%)[b]	24.70
rmsd from restraint values	
bond length (Å)	0.007
bond angle distance (Å)	0.022
Ramachandran analysis	
most favored (%)	89.1
additionally allowed (%)	10.9

[a] $R_{merge} = \Sigma|\langle I\rangle - I|/\Sigma\langle I\rangle$ over all reflections. [b] $R_{cryst} = \Sigma|F_o - F_c|/F_o$; R_{free} calculated with 10.7% data withheld from refinement.

and frozen in liquid nitrogen. A data set was collected to 1.8 Å ($\lambda = 0.87$ Å) on station 9.6 at Daresbury synchrotron source using an ADSC Quantum 4 detector. The crystals are isomorphous with wild-type Fcc_3 with space group $P2_1$ and cell dimensions $a = 45.571$ Å, $b = 92.172$ Å, $c = 78.489$ Å, and $\beta = 91.09°$. This compares with the wild-type crystal cell dimensions of $a = 45.393$ Å, $b = 91.946$ Å, $c = 78.288$ Å, and $\beta = 91.09°$.

Data processing was carried out using the HKL package (*21*) (Table 1). The wild-type Fcc_3 structure (1qjd), stripped of water, was used as the initial model. Electron density fitting was carried out using the graphics program WITNOTP (*22*). Restraints for the heme group were calculated from the CNS parameter file and for the FAD from two small molecule crystal structures (Cambridge Crystallographic Database codes HAMADPH and VEFHUJ10). Structure refinement was carried out using SHELXL-97 (*23*).

The atomic coordinates have been deposited in the Protein Data Bank (accession code 1E39).

RESULTS AND DISCUSSION

Characterization of Recombinant Enzymes. The molecular mass of the recombinant wild-type enzyme was confirmed by electrospray mass spectroscopy to be 63 033 Da. The masses of the mutant enzymes were lower than this by 68 Da for H365A (expected difference 66), 84 Da for R402A (expected difference 85), 59 Da for H504A (expected difference 66), and 134 Da for H365A:H504A (expected difference 132). All the mutations were further verified by DNA sequencing. The average FAD content of the recombinant enzymes was found to be the following: 73%, wild-type; 69%, H365A; 78%, R402A; 70%, H504A; and 68%, H365A:H504A. This compares with typical values for the native (nonrecombinant) enzyme from *Shewanella* of around 98%. The lower flavin content of the recombinant forms is most likely due to the higher levels of expression in these cases. All catalytic rates were corrected for the variation in FAD content.

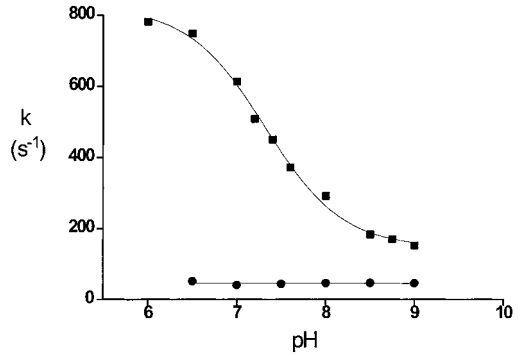

FIGURE 1: pH dependence of fumarate reduction activity (under saturating conditions) at 25 °C: wild-type flavocytochrome c_3 (solid squares); H365A flavocytochrome c_3 (solid circles).

The ability of wild-type and mutant forms of Fcc_3 to catalyze fumarate reduction was determined over a range of pH values. The resulting k_{cat} and K_m parameters for wild-type and mutant forms of Fcc_3 are listed in Table 2. The pH dependence of the rate of fumarate reduction under saturating substrate conditions seen with wild-type and H365A Fcc_3 is shown in Figure 1. The pK_a value seen for the wild-type enzyme is 7.4 ± 0.2, as previously reported (*20*). However, it is clear from the results shown in Figure 1 and Table 2 that the catalytic rate of fumarate reduction seen for the H365A mutant enzyme is essentially independent of pH over the range 6.0−9.0. At pH 6.0 the value of k_{cat} for the H365A enzyme has fallen to approximately 7% of that seen with wild-type Fcc_3. This effect is less dramatic at pH 9.0 where the k_{cat} for the H365A enzyme is 25% of the value seen with the wild-type enzyme. The magnitude of the effect of this mutation on activity is similar to that seen for the His232→Ser mutation made in the *E. coli* enzyme (*9*).

The fact that up to 25% of the value of k_{cat} is retained in the H365A mutant enzyme is not consistent with this residue being an essential active site acid/base catalyst. Rather, we propose that the major role of this residue is in stabilizing the Michaelis complex. This is supported by the values of K_m reported in Table 2. At pH 9.0 the K_m value for the H365A mutant is some 30-fold larger than that seen for the wild-type enzyme. Previous results on the wild-type enzyme from pre-steady-state experiments (*1*) and inhibition studies (*5*) suggest that the K_m for fumarate is similar to the K_d value. We have therefore used the variation in the value of K_m as a means of determining approximate changes in the free energies of fumarate binding between wild-type and mutant enzymes. For example, at pH 9.0 the change in K_m between

Table 2: Comparison of k_{cat} and K_m Values for Wild-Type, H365A, H504A, and the Double Mutant H365A:H504A Fcc_3 (25 °C, $I = 0.45$ M)[a]

	wild-type Fcc_3		H365A Fcc_3		H504A Fcc_3		H365A:H504A Fcc_3	
pH	k_{cat} (s^{-1})	K_m (μM)	k_{cat} (s^{-1})	K_m (μM)	k_{cat} (s^{-1})	K_m (μM)	k_{cat} (s^{-1})	K_m (mM)[b]
6.0	658 ± 34	43 ± 10	47 ± 2	113 ± 20	26 ± 1	38 ± 3	0.28 ± 0.02	∼0.08
7.2	509 ± 15	25 ± 10	51 ± 2	259 ± 24	65 ± 3	256 ± 23	0.84 ± 0.10	∼1.1
7.5	370 ± 10	28 ± 3	54 ± 2	143 ± 21	68 ± 2	200 ± 15	0.95 ± 0.10	∼1.8
9.0	210 ± 13	7.0 ± 1.5	52 ± 2	224 ± 25	76 ± 3	635 ± 37	0.95 ± 0.10	∼1.3

[a] The R402A enzyme was inactive under all conditions. [b] Values of K_m (millimolar) for fumarate with the H365A:H505A enzyme were difficult to determine accurately due the very low activity of the enzyme.

wild-type and H365A enzymes equates to a difference in free energy for the binding of substrate of approximately 8.6 kJ mol^{-1}. In addition, the value of k_{cat}/K_m, a measure of enzyme efficiency, varies between 2×10^5 and 4×10^5 M^{-1} s^{-1} over the pH range 6−9. A catalytic efficiency of 10^5 is typical for many native enzymes and is certainly not consistent with an enzyme in which the key active site acid/base catalyst has been removed.

The possibility of an alternative histidine (His504) acting as the acid/base catalyst has been recently suggested (*10*). However, substitution of this histidine by alanine leads to effects similar to those seen for the H365A mutant enzyme. For H504A Fcc_3 the value of k_{cat} varies from 4% of the wild-type value (at pH 6.0) to 36% of the wild-type value (at pH 9.0). As for H365A, the H504A mutation has large effects on the value of K_m particularly at high pH. For example, at pH 9.0 the K_m value for fumarate seen with the H504A enzyme is some 90-fold larger than that seen for the wild-type enzyme (Table 2), equating to a change in free energy for the binding of substrate of around 11.2 kJ mol^{-1}. Again, it is clear that His504 is not essential for catalysis but is important for Michaelis complex formation.

Even for the case in which both histidines are replaced by alanine (H365A:H504A Fcc_3), there is still some residual activity. Not surprisingly, the double mutation has a large effect on the K_m value for fumarate, with the value now in the millimolar range (Table 2). In fact, the effect of the mutations is additive since, at pH 7.2, the loss in binding energy with respect to wild-type enzyme, seen for the double mutant (∼10 kJ mol^{-1}), is almost exactly the sum of the loss in binding energies for the two single mutants (∼5 kJ mol^{-1}). The effect on k_{cat} is also dramatic (Table 1); however, the fact that there is any activity at all indicates that an alternative acid/base catalyst must still be operating.

These results clearly indicate that a group other than His365 or His504 operates as the crucial proton donor/acceptor. The most likely candidate for this role has previously been suggested to be Arg402 (*7*, *9*). The effect of substituting Arg402 by Ala is far more dramatic than that seen for either of the histidine mutations. In this case the R402A mutant enzyme was found to be completely inactive under all conditions. This abolition of activity is clearly not due to the loss of redox cofactors since the FAD complement was found to be equivalent to that of the recombinant wild-type enzyme. A possible explanation for this abolition of all activity is that Arg402 is indeed the essential active site acid catalyst required for fumarate reduction. This idea is further supported by an inspection of the high-resolution X-ray structure of the wild-type enzyme which shows that the NH2 of Arg402 is ideally positioned for proton donation at only 2.99 Å from the C3 carbon of the substrate (*7*). The mechanism proposed for the reduction of fumarate based on the wild-type enzyme structure (*7*) is shown in Figure 2. This mechanism is shown proceeding in a stepwise rather than in a concerted fashion. The only evidence for the reaction being stepwise comes from the crystallographic identification of a trapped malate-like molecule (an artifact of the crystallization procedure) in the Fcc_3 structure which may represent an unprotonated intermediate (*7*). Clearly, further solution studies will be required to confirm the stepwise nature of the mechanism. Nevertheless, the mechanism shown in Figure 2 is entirely consistent with the roles of His365 and

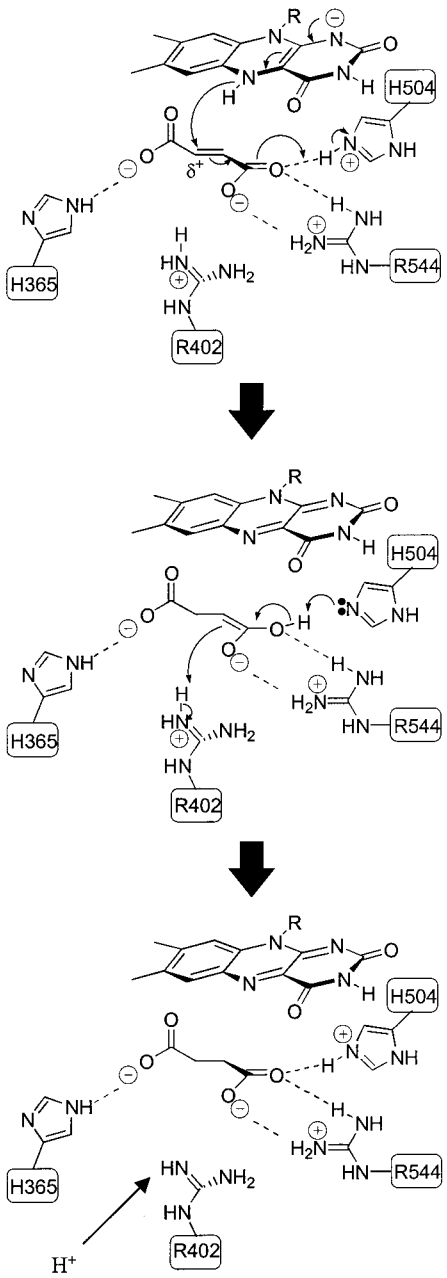

FIGURE 2: Reaction mechanism for fumarate reduction as proposed by Taylor et al. (*7*). Catalysis is initiated by the twisting out of plane of the C1 carboxylate group (on the left) of fumarate. The substrate is polarized by interactions with charged residues facilitating hydride transfer from N5 of reduced FAD to the substrate C2. Arg402 (2.99 Å from C3) is ideally positioned to donate a proton to the substrate C3, resulting in the formation of succinate. Arg402 is immediately reprotonated via a proton pathway involving Arg381 and Glu378 (Figure 3).

Arg402 that we propose on the basis of our mutagenesis results. The mechanism also shows His504 protonating the C4 carboxylate to facilitate the transient formation of a carbanion at C3. While such a role for His504 would clearly facilitate the reaction, it is obviously not essential since removal of the imidazole ring causes only around a 10-fold decrease in the k_{cat} value. It is possible that His504 is the residue with the pK_a of 7.4 observed in the wild-type enzyme. If so, this again shows that a protonated imidazole can enhance the rate of reaction but is not essential for it, since the rate constant at high pH, where the imidazole would be

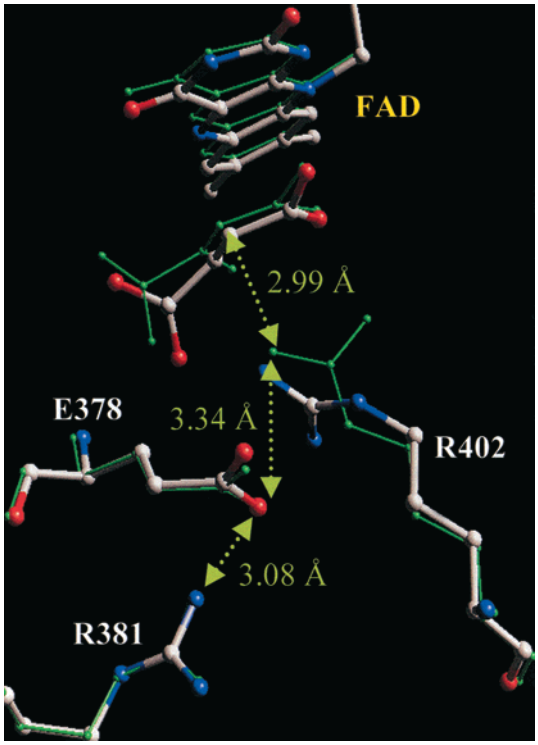

FIGURE 3: Overlay of the structures of wild-type Fcc_3 (green) and H365A Fcc_3 (atom-type colors) showing the proposed proton delivery pathway to the substrate C3 atom involving Arg381, Glu378, and Arg402. The distances indicated are for the wild-type enzyme. The altered conformation of Arg402 in the mutant enzyme is clearly visible.

fully deprotonated, would be around 150 s^{-1} (5−6-fold lower than the value for the fully protonated state).

The use of Arg402 as an active site acid to protonate the substrate clearly requires the guanidine moiety to be reprotonated. Since the active site is completely closed to solvent, we propose that a proton transfer pathway operates involving Arg381, Glu378, and Arg402. This pathway (Figure 3) may facilitate the rapid delivery/removal of protons for catalysis.

The Crystal Structure of H365A Fcc_3. Data to 1.8 Å were used to refine the H365A mutant enzyme structure to a final *R*-factor of 18.1% (Table 1). The final model consists of residues 1−568, 4 hemes, the FAD, 1 substrate molecule, 1 sodium ion, and 584 water molecules. As in wild-type Fcc_3, one *cis*-peptide between Ala175 and Trp176 was clearly identified. The three C-terminal residues (569−571) were not located in the electron density maps. The rmsd fit of all backbone atoms for the wild-type and H365A mutant enzyme is 0.15 Å, showing no significant structural differences between the two structures.

Both wild-type and H365A enzymes were crystallized in the presence of 10 mM fumarate. In the crystal structure of the mutant enzyme, a molecule of fumarate was found at the active site in a twisted conformation (Figure 4). This is in marked contrast to the wild-type structure in which (although found in the same twisted conformation) the molecule at the active site is hydroxylated at the C2 position (*7*).

The active sites of the two structures are compared in Figure 5. A major difference is, of course, the replacement of the histidine by alanine at position 365, removing the original hydrogen bond between His365 N3 and a carboxylate oxygen of the substrate. The removal of this hydrogen bond is entirely consistent with the increased K_m value seen for the mutant enzyme. The void produced by the H365A mutation is compensated by significant changes in side-chain conformations of Met375 and Arg402. Significantly, there is now room for a water molecule which forms a hydrogen bond to the backbone NH of Thr367 (N···O = 3.2 Å). This water is also hydrogen bonded to the side chains of Thr367 (O···O = 2.95 Å) and Arg402 (O···N = 3.14 Å). This latter interaction may contribute toward stabilizing the rather different conformation of the Arg402 side chain, decreasing its effectiveness as a proton donor in fumarate reduction. In other words, the lower activity seen for the mutant enzyme arises from a less favorable orientation for proton donation from Arg402, rather than the loss of the imidazole ring. However, although the side chain of Arg402 has been altered, the closest distance between Arg NH2 and substrate C3 remains at 2.99 Å.

The new conformation of Met375 in the H365A structure also triggers a flip in the orientation of the carbonyl group of Ala169, which swings down, allowing the incorporation of an additional bridging water molecule between A169 (O) and Val253 (N). It is probable that the repositioning of

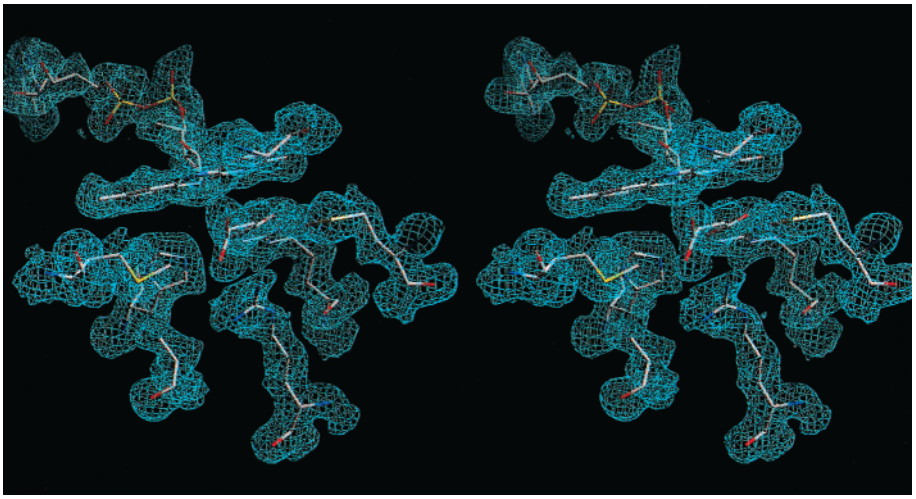

FIGURE 4: Stereoview of the electron density around the active site of the H365A mutant enzyme. The $2F_o - F_c$ map is contoured at the 1.25σ level. The FMN group is clearly visible at the top of the figure with the alanine residue at position 365 at the bottom left and Arg402 at the bottom center.

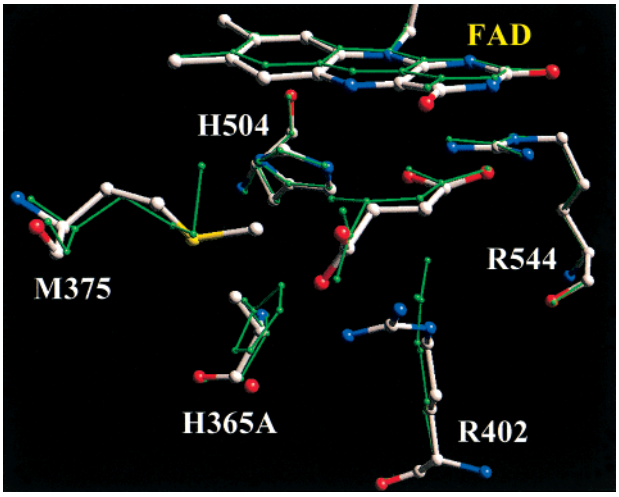

FIGURE 5: Overlay of the structures of wild-type Fcc_3 (green) and H365A Fcc_3 (atom-type colors). The substrate molecule is shown in the center surrounded by key active site residues. The substituted residue is labeled as H365A. Significant shifts in the positions of Met375 and Arg402 can be clearly seen.

Met375 prevents the hydroxylation of fumarate as seen in the wild-type structure, since in the H365A structure, much of the space that would have been taken up by this hydroxyl-group is now occupied by the side chain of Met375.

Comparison with Other Fumarate Reductases. The active sites of each of the known fumarate reductase structures (*3*, *7*−*9*, *24*) are largely well conserved structurally. In all cases, the bound substrate is well positioned to accept a hydride from N5 of the FAD cofactor, and this is clearly a key step in the chemical mechanism of fumarate reduction. The source of the proton needed to complete formation of the product succinate is somewhat less clear from direct observation of the structures and, as already discussed, has been variously proposed to be (using Fcc_3 numbering) His365 (*12*), His504 (*10*), and Arg402 (*7*−*9*). It would be very surprising if these closely related enzymes were to use different proton donors, especially when the residues listed above are conserved in all known fumarate reductases. Prior to the crystallographic results, it was generally expected that a histidine would act as the acid/base catalyst in fumarate reductases and succinate dehydrogenases. This expectation was based on the widespread use of histidines in this role in many types of enzyme and the fact that chemical modification studies with succinate dehydrogenase indicated that a histidine residue played an important catalytic role (*25*). However, results from mutagenesis studies reported in this paper rule out His365 and His504 as the active site acid. In addition, crystallographic analysis shows that His365 and His504 are each hydrogen bonded to substrate carboxylate oxygens and are not well positioned for proton transfer, being too distant from the substrate C3. Thus, the results described here for Fcc_3 confirm the importance of these histidine residues in substrate binding but rule out a key role in substrate protonation.

The structures of two of the *Shewanella* enzymes (*7*, *9*) and *E. coli* fumarate reductase (*3*) clearly show NH2 of Arg402 close to the substrate C3, the eventual proton acceptor. In the structure of the *Wolinella* enzyme, the position of the equivalent arginine (Arg301) has moved by about 3 Å compared to the *Shewanella* and *E. coli* enzyme structures. An overlay of the flavin binding domains of all structures shows that the conserved catalytic residues of the flavin binding domain are very similar. The residues on the clamp domain differ by between 1 and 3 Å, which corresponds to an opening of the clamp in the *Wolinella* structures (*24*). Interestingly, both *Wolinella* structures (with and without fumarate) are similar, though the clamp has closed a little (less than 0.5 Å) when the substrate is present. In addition, the temperature factors of the fumarate and the fumarate binding residues are raised (*24*), suggesting that the protein has been trapped in a partially open conformation. This can be compared to the substrate-free open conformation seen in the structure of the iron-induced flavocytochrome c_3 (*10*). The fact that the arginine side chain is somewhat altered in the *Wolinella* fumarate reductase (*24*) (too distant for efficient proton transfer) has led Lancaster and colleagues to propose that the proton comes instead from a water molecule (*24*). This proposal suffers several weaknesses. The water positioned in the active site of the *Wolinella* enzyme is absent from all other substrate-bound fumarate reductase structures, indicating that if it is used for substrate protonation, then this enzyme is fundamentally different from its close homologues in this key mechanistic aspect. We believe that the equivalent of Arg402 is the true acid catalyst, and we further suggest that if the *Wolinella* enzyme had crystallized in the closed (catalytically active) form, then the position of the arginine side chain would have been comparable to all the other structures.

In conclusion, the combined kinetic and structural evidence strongly suggests that Arg402 is the active site acid catalyst in the fumarate reductase from *Shewanella*. We believe that this conserved arginine residue fulfills this role in all members of the fumarate reductase family.

REFERENCES

1. Pealing, S. L., Cheesman, M. R., Reid, G. A., Thomson, A. J., Ward, F. B., and Chapman, S. K. (1995) *Biochemistry 34*, 6153−6158.
2. Pealing, S. L., Black, A. C., Manson, F. D. C., Ward, F. B., Chapman, S. K., and Reid, G. A. (1992) *Biochemistry 31*, 12132−12140.
3. Iverson, T. M., Luna-Chavez, C., Cecchini, G., and Rees, D. C. (1999) *Science 284*, 1961−1966.
4. Körtner, C., Lauterbach, F., Tripier, D., Unden, G., and Kroger, A. (1990) *Mol. Microbiol. 4*, 855−860.
5. Morris, C. J., Black, A. C., Pealing, S. L., Manson, F. D. C., Chapman, S. K., Reid, G. A., and Ward, F. B. (1994) *Biochem. J. 302*, 587−593.
6. Gordon, E. H. J., Pealing, S. L., Chapman, S. K., Ward, F. B., and Reid, G. A. (1998) *Microbiology 4*, 937−945.
7. Taylor, P., Pealing, S. L., Reid, G. A., Chapman, S. K., and Walkinshaw, M. D. (1999) *Nat. Struct. Biol. 6*, 1108−1112.
8. Chapman, S. K., Morrison, C. A., Reid, G. A., Pealing, S. L., Taylor, P., and Walkinshaw, M. D. (1999) *Flavins Flavoproteins 1999*, 105−113.
9. Leys, D., Tsapin, A. S., Nealson, K. H., Meyer, T. E., Cusanovich, M. A., and Van Beeumen, J. J. (1999) *Nat. Struct. Biol. 6*, 1113−1117.
10. Bamford, V., Dobbin, P. S., Richardson, D. J., and Hemmings, M. (1999) *Nat. Struct. Biol. 6*, 1104−1107.
11. Reid, G. A., Gordon, E. H. J., Hill, A. E., Doherty, M., Turner, K., Holt, R., and Chapman, S. K. (1998) *Biochem. Soc. Trans. 26*, 418−421.
12. Schröder, I., Gunsalus, R. P., Ackrell, B. A. C., Cochran, B., and Cecchini, G. (1991) *J. Biol. Chem. 266*, 13572−13579.
13. Kunkel, T. A., and Roberts, J. D. (1987) *Methods Enzymol. 154*, 367−382.

14. Rokeach, L. A., Haselby, J. A., and Hoch, S. O. (1988) *Proc. Natl. Acad. Sci. U.S.A. 85*, 4832−4836.
15. Sanger, F., Nicklen, S., and Coulson, A. R. (1977) *Proc. Natl. Acad. Sci. U.S.A. 74*, 5463−5467.
16. Michel, L. O., Sandkvist, M., and Bagdasarian, M. (1995) *Gene 152*, 41−45.
17. Simon, R., Priefer, U., and Puhler. A. (1983) *Bio/Technology 1*, 784−791.
18. Pealing, S. L., Lysek, D. A., Taylor, P., Alexeev, D., Reid, G. A., Chapman, S. K., and Walkinshaw, M. D. (1999*) J. Struct. Biol. 127*, 76−78.
19. Macheroux, P. (1999) in *Flavoprotein Protocols: Methods in Molecular Biology* (Chapman, S. K., and Reid, G. A., Eds.) Vol. 131, pp 1−7, Humana Press, Totowa, NJ.
20. Turner, K. L., Doherty, M. K., Heering, H. A., Armstrong, F. A., Reid, G. A., and Chapman, S. K. (1999) *Biochemistry 38*, 3302−3309.
21. Otwinowski, Z., and Minor, W. (1997) *Methods Enzymol. 276*, 307−326.
22. Widmer, A. (1997) Novartis AG, Basel.
23. Sheldrick, G. M. (1997) SHELX-97, University of Goettingen, Germany.
24. Lancaster, C. D., Kröger, A., Auer, M., and Michel, H. (1999) *Nature 402*, 377−385.
25. Vinogradov, A. D. (1986) *Biokhimiya 51*, 1944−1973.

BI000871L